

Correlation of intensity fluctuations in beams generated by quasi-homogeneous sources

Gaofeng Wu^{1,2} and Taco D. Visser^{2,3,*}

¹*School of Physical Science and Technology & Collaborative Innovation Center of Suzhou Nano Science and Technology, Soochow University, Suzhou 215006, China*

²*Department of Physics and Astronomy, and Laserlab, VU University, Amsterdam 1081 HV, The Netherlands*

³*Faculty of Electrical Engineering, Mathematics and Computer Science, Delft University of Technology, Delft 2628 CD, The Netherlands*

*Corresponding author: tviss@nat.vu.nl

Received June 26, 2014; accepted July 27, 2014;
posted August 13, 2014 (Doc. ID 214806); published September 10, 2014

We derive expressions for the far-zone correlation of intensity fluctuations (the Hanbury Brown–Twiss effect) that occurs in electromagnetic beams that are generated by quasi-homogeneous sources. Such sources often have a radiant intensity pattern that is rotationally symmetric, irrespective of the source shape. We demonstrate how from the far-zone correlation of intensity fluctuations the spectral density distribution across the source plane may be reconstructed. © 2014 Optical Society of America

OCIS codes: (030.1640) Coherence; (030.6600) Statistical optics; (050.1960) Diffraction theory; (260.1960) Diffraction theory; (260.2110) Electromagnetic optics.

<http://dx.doi.org/10.1364/JOSAA.31.002152>

1. INTRODUCTION

In the mid-1950s Hanbury Brown and Twiss (HBT) determined the angular diameter of radio stars by analyzing their correlation of intensity fluctuations [1,2]. Since then such correlation measurements have proven to be a powerful tool that can be applied across all branches of physics, see for example, [3–6]. The original description of the HBT effect, which assumes a scalar wave field and is described in [7], was later generalized to electromagnetic beams, see [8] and [9–12]. One major class of partially coherent electromagnetic beams are those generated by so-called Gaussian Schell-model sources [13]. Quite recently two studies were dedicated to the occurrence of the HBT effect in beams of this type [14,15]. Another important class of partially coherent sources, which partially overlaps with those of the Gaussian Schell-model type, is formed by quasi-homogeneous sources. In the space-frequency domain, scalar, secondary, planar quasi-homogeneous sources are characterized by a correlation function, the so-called spectral degree of coherence $\mu^{(0)}(\rho_1, \rho_2, \omega)$ that, at each frequency ω , depends on the source points ρ_1 and ρ_2 only through their difference $\rho_2 - \rho_1$, see Fig. 1. In addition, these sources have a spectral density $S^{(0)}(\rho, \omega)$ that varies much slower with ρ than the modulus of the spectral degree of coherence varies with $\rho_2 - \rho_1$. The properties of quasi-homogeneous sources and those of the far-zone fields they generate, are related by two reciprocity relations. One connects the spectral density of the far field to the spatial Fourier transform of the spectral degree of coherence in the source plane. The other connects the far-zone spectral degree of coherence to the spatial Fourier transform of the spectral density of the source [16–23]. Quite recently, the notion of quasi-homogeneity has been extended to electromagnetic sources, and reciprocity relations have been derived

for the beams that they generate [24]. These relations were then used to illustrate how fundamental field properties, such as the spectrum, polarization, and state of coherence in the far zone, typically differ from those in the source plane. In the present paper we apply these novel reciprocity relations, under the assumption of Gaussian statistics, to study the HBT effect. We derive general expressions for the correlation of intensity fluctuations of the far-zone field, and illustrate our results with several examples. Quasi-homogeneous sources can produce a radiant intensity that is rotationally symmetric, even when the source distribution lacks any symmetry. We demonstrate that the HBT correlations, in contrast to the radiant intensity, provide information about the source shape. For example, in certain cases the aspect ratio of the source can be recovered. Since HBT correlations are obtained from intensity measurements, rather than phase measurements, this provides a reconstruction scheme that is relatively robust to signal degrading factors such as turbulence.

2. CORRELATION OF INTENSITY FLUCTUATIONS OF PARTIALLY COHERENT ELECTROMAGNETIC BEAMS

Let us consider a stochastic, wide-sense stationary, electromagnetic beam propagating close to the z direction into the half space $z > 0$ (see Fig. 1). The source is taken to be the plane $z = 0$. The vector $\rho = (x, y)$ denotes a position in a transverse plane. Let $E_x(\rho, z, \omega)$ and $E_y(\rho, z, \omega)$ be the Cartesian components of the electric field at frequency ω along two mutually orthogonal x and y directions, perpendicular to the beam axis. The intensity of a single realization of the beam at a point (ρ, z) at frequency ω can be expressed as

$$I(\rho, z, \omega) = |E_x(\rho, z, \omega)|^2 + |E_y(\rho, z, \omega)|^2. \quad (1)$$

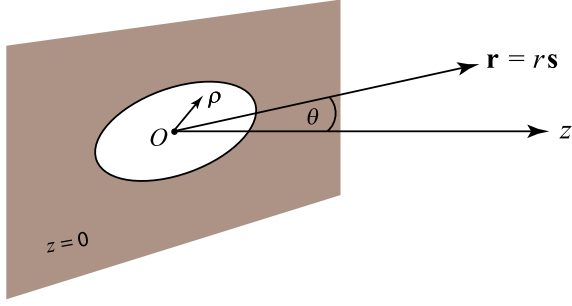


Fig. 1. Illustrating the notation. The origin O of a right-handed Cartesian coordinate system is taken in the source plane $z = 0$. The transverse two-dimensional vector $\boldsymbol{\rho} = (x, y)$ indicates the position of a source point. The position vector \mathbf{r} of a point in the far zone makes an angle θ with the positive z axis. Also, $r = |\mathbf{r}|$, and \mathbf{s} is a directional unit vector.

From now on, we suppress the dependence on the frequency ω in our notation. The intensity is a random quantity, and its variation from its mean value is

$$\Delta I(\boldsymbol{\rho}, z) = I(\boldsymbol{\rho}, z) - \langle I(\boldsymbol{\rho}, z) \rangle, \quad (2)$$

where the angular brackets denote an ensemble average. The statistical properties of such a beam at a pair of points in a cross-sectional plane z are described by the 2×2 cross-spectral density matrix, which is defined as [25]

$$\mathbf{W}(\boldsymbol{\rho}_1, \boldsymbol{\rho}_2, z) = \begin{bmatrix} W_{xx}(\boldsymbol{\rho}_1, \boldsymbol{\rho}_2, z) & W_{xy}(\boldsymbol{\rho}_1, \boldsymbol{\rho}_2, z) \\ W_{yx}(\boldsymbol{\rho}_1, \boldsymbol{\rho}_2, z) & W_{yy}(\boldsymbol{\rho}_1, \boldsymbol{\rho}_2, z) \end{bmatrix}. \quad (3)$$

It follows from this definition that the ensemble-averaged intensity can be expressed as

$$\langle I(\boldsymbol{\rho}, z) \rangle = \text{Tr} \mathbf{W}(\boldsymbol{\rho}, \boldsymbol{\rho}, z), \quad (4)$$

where Tr denotes the trace. The correlation of intensity fluctuations at points $\boldsymbol{\rho}_1$ and $\boldsymbol{\rho}_2$ in the same cross-sectional plane z is defined as

$$C(\boldsymbol{\rho}_1, \boldsymbol{\rho}_2, z) = \langle \Delta I(\boldsymbol{\rho}_1, z) \Delta I(\boldsymbol{\rho}_2, z) \rangle. \quad (5)$$

We assume that the random fluctuations of the source are governed by a Gaussian process. It then follows, by use of the Gaussian moment theorem, that the correlation of intensity fluctuations may be expressed in terms of elements of the cross-spectral density matrix as [8]

$$C(\boldsymbol{\rho}_1, \boldsymbol{\rho}_2, z) = \sum_{ij} |W_{ij}(\boldsymbol{\rho}_1, \boldsymbol{\rho}_2, z)|^2, \quad (i, j = x, y). \quad (6)$$

3. QUASI-HOMOGENEOUS, SECONDARY PLANAR ELECTROMAGNETIC SOURCES

In this section we establish our notation and briefly review some recently derived reciprocity relations.

The elements of the cross-spectral density matrix in the source plane can be written in the form [7]

$$W_{ij}^{(0)}(\boldsymbol{\rho}_1, \boldsymbol{\rho}_2) = \sqrt{S_i^{(0)}(\boldsymbol{\rho}_1) S_j^{(0)}(\boldsymbol{\rho}_2)} \mu_{ij}^{(0)}(\boldsymbol{\rho}_2 - \boldsymbol{\rho}_1), \quad (i, j = x, y), \quad (7)$$

where $S_i^{(0)}(\boldsymbol{\rho}) = \langle |E_i(\boldsymbol{\rho})|^2 \rangle$ denotes the spectral density associated with the Cartesian component E_i of the electric field vector in the plane $z = 0$. Its two-dimensional spatial Fourier transform is defined as

$$\tilde{S}_i^{(0)}(\mathbf{f}) = \frac{1}{(2\pi)^2} \int_{z=0} S_i^{(0)}(\boldsymbol{\rho}) \exp(-i\mathbf{f} \cdot \boldsymbol{\rho}) d^2\rho. \quad (8)$$

We also introduce the function

$$S_{xy}^{(0)}(\boldsymbol{\rho}) = \sqrt{S_x^{(0)}(\boldsymbol{\rho})} \sqrt{S_y^{(0)}(\boldsymbol{\rho})}, \quad (9)$$

and its Fourier transform

$$\tilde{S}_{xy}^{(0)}(\mathbf{f}) = \frac{1}{(2\pi)^2} \int_{z=0} \sqrt{S_x^{(0)}(\boldsymbol{\rho})} \sqrt{S_y^{(0)}(\boldsymbol{\rho})} \exp(-i\mathbf{f} \cdot \boldsymbol{\rho}) d^2\rho. \quad (10)$$

Similarly, the spatial Fourier transform of the four correlation coefficients $\mu_{ij}^{(0)}(\boldsymbol{\rho})$ is given by the expression

$$\tilde{\mu}_{ij}^{(0)}(\mathbf{f}) = \frac{1}{(2\pi)^2} \int_{z=0} \mu_{ij}^{(0)}(\boldsymbol{\rho}) \exp(-i\mathbf{f} \cdot \boldsymbol{\rho}) d^2\rho. \quad (11)$$

In [24] it was derived that for a planar, secondary quasi-homogeneous source, the elements of the cross-spectral density matrix in the far zone, labeled by the superscript (∞) , are connected to the source properties, labeled by the superscript (0) , through the reciprocity relations

$$\begin{aligned} W_{xx}^{(\infty)}(r_1 \mathbf{s}_1, r_2 \mathbf{s}_2) &= (2\pi k)^2 \cos \theta_1 \cos \theta_2 \frac{e^{ik(r_2 - r_1)}}{r_2 r_1} \\ &\times \tilde{S}_x^{(0)}[k(\mathbf{s}_{2\perp} - \mathbf{s}_{1\perp})] \tilde{\mu}_{xx}^{(0)}[k(\mathbf{s}_{2\perp} + \mathbf{s}_{1\perp})/2], \end{aligned} \quad (12)$$

$$\begin{aligned} W_{xy}^{(\infty)}(r_1 \mathbf{s}_1, r_2 \mathbf{s}_2) &= (2\pi k)^2 \cos \theta_1 \cos \theta_2 \frac{e^{ik(r_2 - r_1)}}{r_2 r_1} \\ &\times \tilde{S}_{xy}^{(0)}[k(\mathbf{s}_{2\perp} - \mathbf{s}_{1\perp})] \tilde{\mu}_{xy}^{(0)}[k(\mathbf{s}_{2\perp} + \mathbf{s}_{1\perp})/2], \end{aligned} \quad (13)$$

$$\begin{aligned} W_{yx}^{(\infty)}(r_1 \mathbf{s}_1, r_2 \mathbf{s}_2) &= (2\pi k)^2 \cos \theta_1 \cos \theta_2 \frac{e^{ik(r_2 - r_1)}}{r_2 r_1} \\ &\times \tilde{S}_{xy}^{(0)*}[k(\mathbf{s}_{2\perp} - \mathbf{s}_{1\perp})] \tilde{\mu}_{yx}^{(0)*}[k(\mathbf{s}_{2\perp} + \mathbf{s}_{1\perp})/2], \end{aligned} \quad (14)$$

$$\begin{aligned} W_{yy}^{(\infty)}(r_1 \mathbf{s}_1, r_2 \mathbf{s}_2) &= (2\pi k)^2 \cos \theta_1 \cos \theta_2 \frac{e^{ik(r_2 - r_1)}}{r_2 r_1} \\ &\times \tilde{S}_y^{(0)}[k(\mathbf{s}_{2\perp} - \mathbf{s}_{1\perp})] \tilde{\mu}_{yy}^{(0)}[k(\mathbf{s}_{2\perp} + \mathbf{s}_{1\perp})/2], \end{aligned} \quad (15)$$

where $k = 2\pi/\lambda$ is the wavenumber associated with wavelength λ , and $\mathbf{s}_{\alpha\perp} = (\sin \theta_\alpha \cos \phi_\alpha, \sin \theta_\alpha \sin \phi_\alpha)$ is the two-dimensional projection of the directional unit vector \mathbf{s}_α onto the xy plane ($\alpha = 1, 2$). Furthermore, θ_α is the angle between \mathbf{s}_α and the positive z axis, and ϕ_α is the azimuthal angle in the xy plane.

The radiant intensity of the beam is defined as [8]

$$J(rs) = r^2 \text{Tr } \mathbf{W}^{(\infty)}(rs, rs), \quad (16)$$

$$= (2\pi k \cos \theta)^2 [\tilde{S}_x^{(0)}(0) \tilde{\mu}_{xx}^{(0)}(ks_{\perp}) + \tilde{S}_y^{(0)}(0) \tilde{\mu}_{yy}^{(0)}(ks_{\perp})]. \quad (17)$$

It is seen from Eq. (17) that if the functions $\tilde{\mu}_{xx}^{(0)}(ks_{\perp})$ and $\tilde{\mu}_{yy}^{(0)}(ks_{\perp})$ are both rotationally symmetric, i.e., if they only depend on $|ks_{\perp}|$, then the radiant intensity is rotationally symmetric about the normal to the source plane, irrespective of the spectral density distribution of the source. As we will see in Section 6, it is possible to construct sources whose radiant intensities have rotational symmetry, but whose correlation of intensity fluctuations lack such symmetry.

4. BEAM CONDITIONS FOR QUASI-HOMOGENEOUS SOURCES

In order that the field generated by a quasi-homogeneous source is beam-like, the radiant intensity $J(rs)$ must be negligible except when the unit vector \mathbf{s} lies in a narrow solid angle about the z axis. It follows from Eq. (17) that this will be the case when both

$$|\tilde{\mu}_{xx}^{(0)}(ks_{\perp})| \approx 0, \quad (18)$$

$$|\tilde{\mu}_{yy}^{(0)}(ks_{\perp})| \approx 0, \quad (19)$$

unless $s_{\perp}^2 \ll 1$. To illustrate these two conditions, we consider a quasi-homogeneous source whose diagonal correlation coefficients are both Gaussian, i.e.,

$$\mu_{xx}^{(0)}(\rho) = \exp\left(-\frac{\rho^2}{2\delta_{xx}^2}\right), \quad (20)$$

$$\mu_{yy}^{(0)}(\rho) = \exp\left(-\frac{\rho^2}{2\delta_{yy}^2}\right). \quad (21)$$

In that case,

$$\tilde{\mu}_{xx}^{(0)}(ks_{\perp}) = \frac{\delta_{xx}^2}{2\pi} \exp\left(-\frac{\delta_{xx}^2 k^2 s_{\perp}^2}{2}\right), \quad (22)$$

$$\tilde{\mu}_{yy}^{(0)}(ks_{\perp}) = \frac{\delta_{yy}^2}{2\pi} \exp\left(-\frac{\delta_{yy}^2 k^2 s_{\perp}^2}{2}\right). \quad (23)$$

Equations (18) and (19) are clearly satisfied if both

$$\delta_{xx} \gg \frac{\lambda}{\pi\sqrt{2}}, \quad (24)$$

$$\delta_{yy} \gg \frac{\lambda}{\pi\sqrt{2}}. \quad (25)$$

These two beam conditions are a generalization of the result for scalar fields that was derived in [8].

5. CORRELATION OF INTENSITY FLUCTUATIONS

On substituting from Eqs. (12)–(15) into Eq. (6), we obtain for the correlation of intensity fluctuations in the far zone the expression

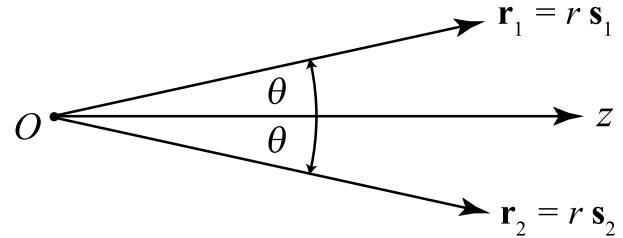


Fig. 2. Two far-zone observation points \mathbf{r}_1 and \mathbf{r}_2 that are symmetrically located with respect to the z axis.

$$C^{(\infty)}(r_1 \mathbf{s}_1, r_2 \mathbf{s}_2) = \left[\frac{(2\pi k)^2 \cos \theta_1 \cos \theta_2}{r_1 r_2} \right]^2 \times \{ |\tilde{S}_x^{(0)}[k(\mathbf{s}_{2\perp} - \mathbf{s}_{1\perp})] \tilde{\mu}_{xx}^{(0)}[k(\mathbf{s}_{2\perp} + \mathbf{s}_{1\perp})/2] |^2 + 2 |\tilde{S}_{xy}^{(0)}[k(\mathbf{s}_{2\perp} - \mathbf{s}_{1\perp})] \tilde{\mu}_{xy}^{(0)}[k(\mathbf{s}_{2\perp} + \mathbf{s}_{1\perp})/2] |^2 + |\tilde{S}_y^{(0)}[k(\mathbf{s}_{2\perp} - \mathbf{s}_{1\perp})] \tilde{\mu}_{yy}^{(0)}[k(\mathbf{s}_{2\perp} + \mathbf{s}_{1\perp})/2] |^2 \}. \quad (26)$$

We introduce a normalized correlation of intensity fluctuations, labeled by the subscript N , by defining

$$C_N^{(\infty)}(r_1 \mathbf{s}_1, r_2 \mathbf{s}_2) = \frac{C^{(\infty)}(r_1 \mathbf{s}_1, r_2 \mathbf{s}_2)}{\langle I^{(\infty)}(r_1 \mathbf{s}_1) \rangle \langle I^{(\infty)}(r_2 \mathbf{s}_2) \rangle}, \quad (27)$$

where

$$\begin{aligned} \langle I^{(\infty)}(r_\alpha \mathbf{s}_\alpha) \rangle &= \text{Tr } \mathbf{W}^{(\infty)}(r_\alpha \mathbf{s}_\alpha, r_\alpha \mathbf{s}_\alpha) \\ &= \left(\frac{2\pi k \cos \theta_\alpha}{r_\alpha} \right)^2 [\tilde{S}_x^{(0)}(0) \tilde{\mu}_{xx}^{(0)}(ks_{\alpha\perp}) \\ &\quad + \tilde{S}_y^{(0)}(0) \tilde{\mu}_{yy}^{(0)}(ks_{\alpha\perp})], \quad (\alpha = 1, 2). \end{aligned} \quad (28)$$

From now on we consider pairs of observation points that are located symmetrically with respect to the z axis (see Fig. 2), i.e., we set $r_1 = r_2 = r$; $\mathbf{s}_{1\perp} = -\mathbf{s}_{2\perp} = -\mathbf{s}_{\perp}$, and $\theta_1 = \theta_2 = \theta$.

Since the four correlation coefficients $\mu_{ij}^{(0)}$ are “fast” functions of their argument, their Fourier transforms $\tilde{\mu}_{ij}^{(0)}$ will be “slow” functions. Hence, we may write

$$\tilde{\mu}_{ij}^{(0)}(ks_{1\perp}) \approx \tilde{\mu}_{ij}^{(0)}(ks_{2\perp}) \approx \tilde{\mu}_{ij}^{(0)}\left[\frac{k(\mathbf{s}_{2\perp} + \mathbf{s}_{1\perp})}{2}\right] = \tilde{\mu}_{ij}^{(0)}(0). \quad (29)$$

On making use of these approximations in Eq. (27), we find for the normalized correlation of intensity fluctuations the formula

$$\begin{aligned} C_N^{(\infty)}(r \mathbf{s}_1, r \mathbf{s}_2) &= \{ |\tilde{S}_x^{(0)}(2k\mathbf{s}_{\perp}) \tilde{\mu}_{xx}^{(0)}(0) |^2 + 2 |\tilde{S}_{xy}^{(0)}(2k\mathbf{s}_{\perp}) \tilde{\mu}_{xy}^{(0)}(0) |^2 \\ &\quad + |\tilde{S}_y^{(0)}(2k\mathbf{s}_{\perp}) \tilde{\mu}_{yy}^{(0)}(0) |^2 \} \\ &\quad \times [\tilde{S}_x^{(0)}(0) \tilde{\mu}_{xx}^{(0)}(0) + \tilde{S}_y^{(0)}(0) \tilde{\mu}_{yy}^{(0)}(0)]^{-2}, \\ &\quad (r_1 = r_2 = r; \mathbf{s}_{1\perp} = -\mathbf{s}_{2\perp} = -\mathbf{s}_{\perp}). \end{aligned} \quad (30)$$

We will employ Eq. (30) to investigate the HBT effect for different kinds of sources.

6. EXAMPLES

Let us first consider an unpolarized, quasi-homogeneous source with an arbitrary shape. In that case we have

$$S_x^{(0)}(\boldsymbol{\rho}) = S_y^{(0)}(\boldsymbol{\rho}) = S^{(0)}(\boldsymbol{\rho}), \quad (31)$$

$$\mu_{xy}^{(0)}(\boldsymbol{\rho}) = 0. \quad (32)$$

We note that for an unpolarized source it is not necessary to have $\mu_{xx}^{(0)}(\boldsymbol{\rho}) = \mu_{yy}^{(0)}(\boldsymbol{\rho})$, see also the discussion in [26]. Substitution from Eqs. (31) and (32) into Eq. (30) yields the expression

$$C_N^{(\infty)}(r\mathbf{s}_1, r\mathbf{s}_2) = \frac{|\tilde{\mu}_{xx}^{(0)}(0)|^2 + |\tilde{\mu}_{yy}^{(0)}(0)|^2}{[\tilde{S}^{(0)}(0)]^2 [|\tilde{\mu}_{xx}^{(0)}(0)| + |\tilde{\mu}_{yy}^{(0)}(0)|]^2} |\tilde{S}^{(0)}(2k\mathbf{s}_\perp)|^2. \quad (33)$$

This result shows that for any planar, secondary quasi-homogeneous, unpolarized source the normalized correlation of intensity fluctuations between two symmetrically located far-zone points is proportional to $|\tilde{S}^{(0)}(2k\mathbf{s}_\perp)|^2$, i.e., to the squared modulus of the Fourier transform of the source spectral density at spatial frequency $2k\mathbf{s}_\perp$.

Next, we consider the case of a disk-shaped source of radius a with two (possibly different) uniform spectral densities, and with Gaussian correlation coefficients, i.e.,

$$S_i^{(0)}(\boldsymbol{\rho}) = A_i^2 \text{circ}(\rho/a), \quad (34)$$

where the circle function

$$\text{circ}(\rho) = \begin{cases} 1 & \text{if } |\rho| \leq 1, \\ 0 & \text{if } |\rho| > 1, \end{cases} \quad (35)$$

and

$$\mu_{ij}^{(0)}(\boldsymbol{\rho}) = B_{ij} \exp\left(-\frac{\rho^2}{2\delta_{ij}^2}\right), \quad (i, j = x, y). \quad (36)$$

The assumption of quasi-homogeneity implies that $a \gg \delta_{ij}$, for all i, j . The parameters A_i , B_{ij} , and δ_{ij} are independent of position, but may depend on the frequency ω . They cannot be chosen arbitrarily. In particular [7],

$$B_{xx} = B_{yy} = 1, \quad (37)$$

$$B_{xy} = B_{yx}^*, \quad (38)$$

$$|B_{xy}| \leq 1, \quad (39)$$

$$\delta_{xy} = \delta_{yx}. \quad (40)$$

To ensure that the source generates a beam-like field, the two correlation lengths δ_{xx} and δ_{yy} must satisfy the conditions (24) and (25). Finally, in order for the source to be physically realizable, its cross-spectral density matrix must be positive definite. This implies that [27]

$$\sqrt{\frac{\delta_{xx}^2 + \delta_{yy}^2}{2}} \leq \delta_{xy} \leq \sqrt{\frac{\delta_{xx}\delta_{yy}}{|B_{xy}|}}. \quad (41)$$

[Note that although Eq. (41) is derived in [27] in the context of Gaussian Schell-model sources, it only depends on the properties of the correlation coefficients and not on those of the

spectral density of the source. It therefore applies to our example.] In the present case the relevant Fourier transforms are

$$\tilde{S}_i^{(0)}(\mathbf{f}) = \frac{A_i^2 a^2 J_1(af)}{2\pi af}, \quad (42)$$

$$\tilde{S}_{xy}^{(0)}(\mathbf{f}) = \frac{A_x A_y a^2 J_1(af)}{2\pi af}, \quad (43)$$

$$\tilde{\mu}_{ij}^{(0)}(\mathbf{f}) = \frac{B_{ij} \delta_{ij}^2}{2\pi} \exp\left(-\frac{\delta_{ij}^2 f^2}{2}\right), \quad (44)$$

where $f = |\mathbf{f}|$ and J_1 is the Bessel function of the first kind and first order. On substituting from Eqs. (42)–(44) into Eq. (30), we find that

$$C_N^{(\infty)}(r\mathbf{s}_1, r\mathbf{s}_2) = 4D \left[\frac{J_1(2ka \sin \theta)}{2ka \sin \theta} \right]^2 \quad (45)$$

with

$$D = \frac{\sum_{i,j} A_i^2 A_j^2 |B_{ij}|^2 \delta_{ij}^4}{(A_x^2 \delta_{xx}^2 + A_y^2 \delta_{yy}^2)^2}, \quad (46)$$

and where we have made the use of the fact that $|\mathbf{s}_\perp| = \sin \theta$. From Eqs. (45) and (46) it is seen that $C_N^{(\infty)}(r\mathbf{s}_1, r\mathbf{s}_2)$ is rotationally symmetric about the z axis. We notice that the off-diagonal coefficient B_{xy} only appears in the numerator of the function D . That means that an unpolarized, quasi-homogeneous source with $|B_{xy}| = 0$ has a weaker correlation of its intensity fluctuations than a partially polarized source with $|B_{xy}| \neq 0$. This is shown in Fig. 3 where $C_N^{(\infty)}(r\mathbf{s}_1, r\mathbf{s}_2)$ is plotted for selected values of $|B_{xy}|$. When this parameter is nearing its upper value (blue curve), which can be calculated from Eq. (41), the maximum value of $C_N^{(\infty)}(r\mathbf{s}_1, r\mathbf{s}_2)$ almost reaches unity.

Another parameter that significantly influences the far-zone correlations is the ratio of the two spectral amplitudes A_x and A_y . Examples are shown in Fig. 4. When $A_y \gg A_x$, i.e., approaching the case of a y -polarized source, the correlation

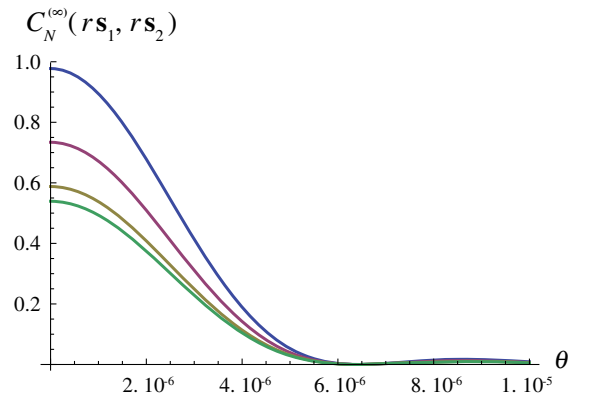


Fig. 3. Variation of the normalized correlation of intensity fluctuations in the far zone, as a function of the observation angle θ for different values of $|B_{xy}|$. From top to bottom: $|B_{xy}| = 0.9$ (blue), 0.6 (purple), 0.3 (olive), 0 (green). In this example $a = 3$ cm, $\delta_{xx} = 0.4$ mm, $\delta_{xy} = 0.51$ mm, $\delta_{yy} = 0.6$ mm, $A_x = 2$, $A_y = 1$, and $\lambda = 632.8$ nm.

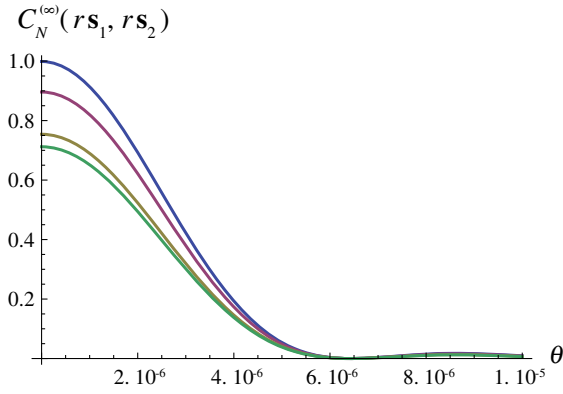


Fig. 4. Variation of the normalized correlation of intensity fluctuations in the far zone as a function of θ for different values of the spectral amplitude A_y , with A_x kept fixed at 1. From top to bottom: $A_y = 20$ (blue), 2 (purple), 1 (olive), 0.7 (green). In this example, $A_x = 1$, $a = 3$ cm, $\delta_{xx} = 0.4$ mm, $\delta_{xy} = 0.51$ mm, $\delta_{yy} = 0.6$ mm, $|B_{xy}| = 0.6$, and $\lambda = 632.8$ nm.

reaches its maximum value of unity at $\theta = 0^\circ$. The curve decreases with decreasing A_y until this spectral amplitude reaches about 0.7. For lower values the correlation of intensity fluctuations rises again, as the source becomes more and more like a linear polarized source, but now with its main polarization along x .

Let us next consider a source with a rectangular shape, with sides a and b , with two uniform spectral densities, and with Gaussian correlation coefficients. In that case we have

$$S_i^{(0)}(\boldsymbol{\rho}) = A_i^2 \text{rect}(x/a)\text{rect}(y/b), \tag{47}$$

with the rectangle function

$$\text{rect}(x) = \begin{cases} 1 & \text{if } |x| \leq 1/2, \\ 0 & \text{if } |x| > 1/2, \end{cases} \tag{48}$$

and

$$\mu_{ij}^{(0)}(\boldsymbol{\rho}) = B_{ij} \exp\left(-\frac{\rho^2}{2\delta_{ij}^2}\right). \tag{49}$$

The assumption of quasi-homogeneity implies that $a \gg \delta_{ij}$ and $b \gg \delta_{ij}$, for all i, j . The parameters A_i, B_{ij} , and δ_{ij} satisfy the same constraints as in the previous example. The pertinent Fourier transforms are now

$$\tilde{S}_i^{(0)}(\mathbf{f}) = ab \left(\frac{A_i}{2\pi}\right)^2 \text{sinc}\left(\frac{f_x a}{2}\right) \text{sinc}\left(\frac{f_y b}{2}\right), \tag{50}$$

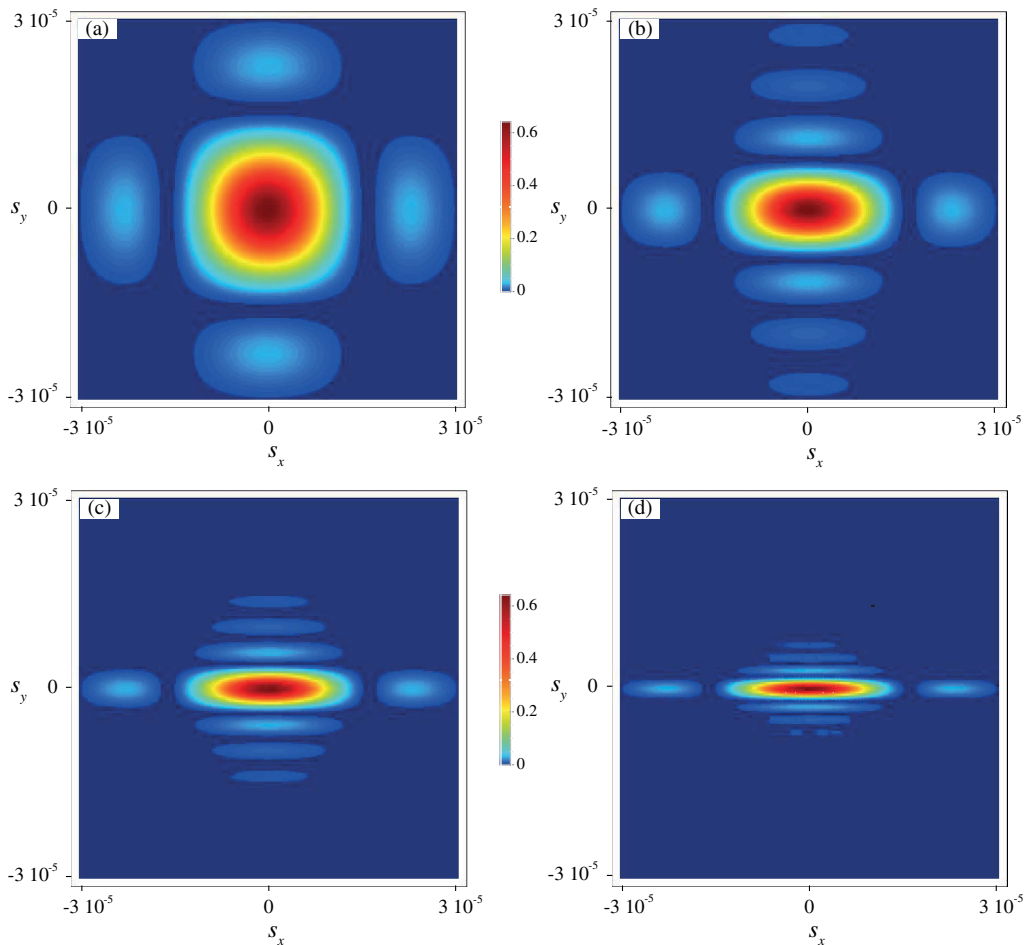


Fig. 5. Contours of the normalized correlation of intensity fluctuations of beams generated by rectangular sources with sides a and b . The sides are chosen as (a) $b = a$, (b) $b = 2a$, (c) $b = 4a$, and (d) $b = 8a$. In these examples $A_x = 2$, $A_y = 1$, $B_{xy} = 0.2$, $\delta_{xx} = 0.4$ mm, $\delta_{yy} = 0.6$ mm, $\delta_{xy} = 0.75$ mm, $a = 2$ cm, and $\lambda = 632.8$ nm.

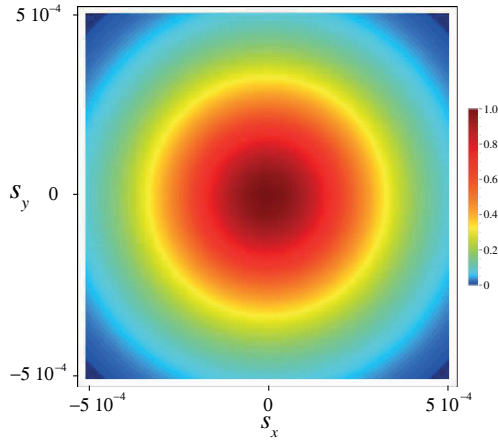


Fig. 6. Contours of the normalized radiant intensity of beams generated by rectangular sources. The parameters are the same as in Fig. 5.

$$\tilde{S}_{xy}^{(0)}(\mathbf{f}) = ab \frac{A_x A_y}{(2\pi)^2} \text{sinc}\left(\frac{f_x a}{2}\right) \text{sinc}\left(\frac{f_y b}{2}\right), \quad (51)$$

$$\tilde{\mu}_{ij}^{(0)}(\mathbf{f}) = \frac{B_{ij} \delta_{ij}^2}{2\pi} \exp\left(-\frac{\delta_{ij}^2 f^2}{2}\right), \quad (52)$$

where $\mathbf{f} = (f_x, f_y)$. On substituting from Eqs. (50)–(52) into Eq. (30), we find for the far-zone correlation of intensity fluctuations of a rectangular source the expression

$$C_N^{(\infty)}(r\mathbf{s}_1, r\mathbf{s}_2) = D \text{sinc}^2(kas_x) \text{sinc}^2(kbs_y), \quad (53)$$

with the function D defined by Eq. (46), and with the two directions of observation set to $\mathbf{s}_1 = (s_x, s_y, s_z)$, $\mathbf{s}_2 = (-s_x, -s_y, s_z)$. Examples of the correlation function for rectangular sources with different aspect ratios a/b are shown in Fig. 5. Clearly, these patterns indicate the symmetry properties of the four sources along the s_x and s_y axes.

It is interesting to compare the contours of $C_N^{(\infty)}(r\mathbf{s}_1, r\mathbf{s}_2)$ with those of the radiant intensity. From Eq. (17) we have that

$$J(r\mathbf{s}) = \frac{abk^2}{2\pi} (1 - s_x^2 - s_y^2) [A_x^2 \delta_{xx}^2 e^{-\delta_{xx}^2 k^2 (s_x^2 + s_y^2)/2} + A_y^2 \delta_{yy}^2 e^{-\delta_{yy}^2 k^2 (s_x^2 + s_y^2)/2}]. \quad (54)$$

The normalized radiant intensity $J(r\mathbf{s})/J(0)$ is plotted in Fig. 6. This far-field radiation pattern has rotational symmetry, and is independent of the aspect ratio a/b of the rectangular source: it contains no information about the shape of the source or its spectral density distribution. This is in contrast to the

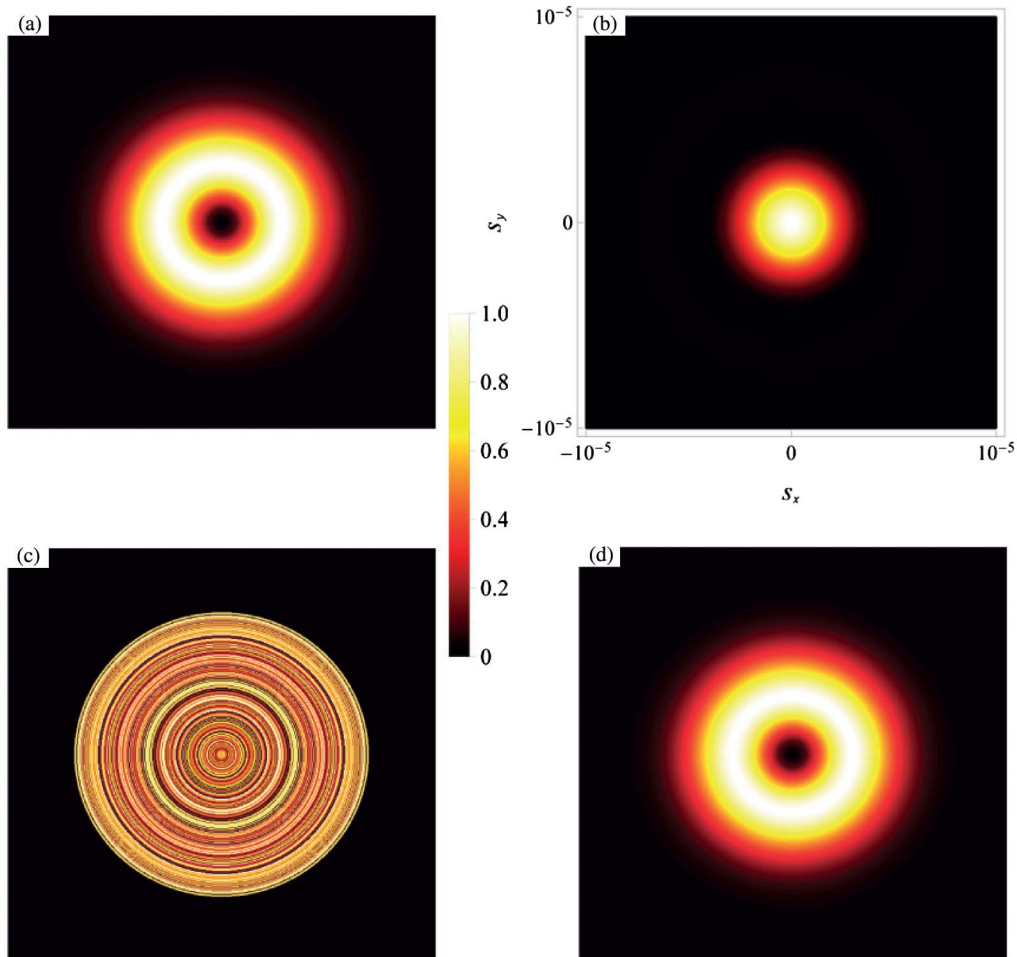


Fig. 7. Retrieval of a simulated spectral density from its normalized correlation of intensity fluctuations in the far-zone. (a) The spectral density of a partially coherent Laguerre–Gauss beam in the source plane. In this example $\lambda = 632.8$ nm and $\sigma_x = 15$ mm. (b) The normalized correlation of intensity fluctuations in the far zone. (c) The initial guess for the source spectral density that is used to start the algorithm: a completely random pattern with rotational symmetry and with values between 0 and 1. (d) The result of the reconstructed source spectral density after 80 iterations.

correlation of intensity fluctuations $C_N^{(\infty)}(r\mathbf{s}_1, r\mathbf{s}_2)$, which, as can be seen from Eq. (30), provides the modulus of the spatial Fourier transform of the spectral density distribution in the source plane in this particular case. There is a large body of literature devoted to phase retrieval, i.e., the reconstruction of an object by knowledge of the modulus of its Fourier transform, see [28] and the references therein. We demonstrate the feasibility of using the correlation of intensity fluctuations for this purpose with a simple example. Consider a partially coherent Laguerre–Gauss beam, with Gaussian correlation coefficients. Let two linear polarizers that only transmit x -polarized fields cover the intensity detectors. The relevant spectral density and the autocorrelation coefficient are then

$$S_x^{(0)}(\rho) = A_x^2 \rho^2 \exp(-\rho^2/2\sigma_x^2), \quad (55)$$

$$\mu_{xx}^{(0)}(\rho) = \exp(-\rho^2/2\delta_{xx}^2), \quad (56)$$

with σ_x the effective width of the spectral density, and δ_{xx} the effective correlation length. The assumption of quasi-homogeneity implies that $\sigma_x \gg \delta_{xx}$. Under these assumptions Eq. (30) reduces to the form

$$C_N^{(\infty)}(r\mathbf{s}_1, r\mathbf{s}_2) = \frac{|\tilde{S}_x^{(0)}(2k\mathbf{s}_\perp)|^2}{[\tilde{S}_x^{(0)}(0)]^2}, \quad (r_1 = r_2 = r; \mathbf{s}_{1\perp} = -\mathbf{s}_{2\perp} = -\mathbf{s}_\perp). \quad (57)$$

Since

$$\tilde{S}_x^{(0)}(\mathbf{f}) = (2 - f^2 \sigma_x^2) \sigma_x^4 A_x^2 \exp(-f^2 \sigma_x^2/2)/2\pi, \quad (58)$$

we obtain the expression

$$C_N^{(\infty)}(r\mathbf{s}_1, r\mathbf{s}_2) = (1 - 2k^2 \sigma_x^2 \sin^2 \theta)^2 \exp(-4k^2 \sigma_x^2 \sin^2 \theta). \quad (59)$$

The iterative method proposed in [29] was used to reconstruct the spectral density distribution across the source plane from Eq. (59). The principal constraint for each iteration being that the object is nonnegative. The contours of the spectral density $S_x^{(0)}(\rho)$ and those of the correlation of intensity fluctuations $C_N^{(\infty)}(r\mathbf{s}_1, r\mathbf{s}_2)$ are plotted in panels (a) and (b) of Fig. 7. From the shape of the correlation function it is seen that the source is rotationally symmetric. The initial “guess” that is used to start the iteration process is therefore taken as a random pattern with rotational symmetry, shown in panel c. The reconstructed source spectral density after 80 iterations is shown in panel d. It is seen to be very similar to the original spectral density of panel a. By rotating the two linear polarizers that cover the detectors, the distribution of $S_y^{(0)}(\rho)$ can be reconstructed in a completely similar way.

Previously proposed methods to reconstruct the source spectral density of quasi-homogeneous sources rely on far-zone measurements of the spectral degree of coherence, see [8]. However, such interference experiments are quite difficult to carry out. On the other hand, measuring the correlation function $C_N^{(\infty)}(r\mathbf{s}_1, r\mathbf{s}_2)$ involves intensity measurements that are typically more robust to noise. The inversion scheme as described above may therefore offer a more practical approach for inverse imaging problems.

7. CONCLUSION

We have studied the correlation of intensity fluctuations in the far zone that occurs in electromagnetic beams generated by quasi-homogeneous sources. The influence of the different source parameters was investigated numerically. We found that the aspect ratio of rectangular sources with a homogeneous intensity may be determined from the correlation of intensity fluctuations. We also showed that the spectral density distribution in the source plane can be reconstructed from measurements of the HBT effect. This approach may find application in remote sensing and imaging.

ACKNOWLEDGMENTS

G. W. would like to thank the China Scholarship Council and the Priority Academic Program Development of Jiangsu Higher Education Institutions for their support.

REFERENCES

1. R. Hanbury Brown and R. Q. Twiss, “A new type of interferometer for use in radio astronomy,” *Philos. Mag.* **45**(366), 663–682 (1954).
2. R. Hanbury Brown and R. Q. Twiss, “Correlation between photons in two coherent beams of light,” *Nature* **177**, 27–29 (1956).
3. G. Baym, “The physics of Hanbury Brown–Twiss intensity interferometry: from stars to nuclear collisions,” *Acta Phys. Pol. B* **29**, 1839–1884 (1998).
4. A. Öttl, S. Ritter, M. Köhl, and T. Esslinger, “Correlations and counting statistics of an atom laser,” *Phys. Rev. Lett.* **95**, 090404 (2005).
5. M. Schellekens, R. Hoppeler, A. Perrin, J. V. Gomes, D. Boiron, A. Aspect, and C. I. Westbrook, “Hanbury Brown–Twiss effect for ultracold quantum gases,” *Science* **310**, 648–651 (2005).
6. D. Kuebel, T. D. Visser, and E. Wolf, “Application of the Hanbury Brown–Twiss effect to scattering from quasi-homogeneous media,” *Opt. Commun.* **294**, 43–48 (2013).
7. E. Wolf, *Introduction to the Theory of Coherence and Polarization of Light* (Cambridge University, 2007), Chap. 7, Chap. 9, Chap. 9.4.2.
8. L. Mandel and E. Wolf, *Optical Coherence and Quantum Optics* (Cambridge University, 1995), Chap. 8, Sect. 5.2, Sect. 5.3.3, Sect. 5.6.4.
9. T. Shirai and E. Wolf, “Correlations between intensity fluctuations in stochastic electromagnetic beams of any state of coherence and polarization,” *Opt. Commun.* **272**, 289–292 (2007).
10. S. N. Volkov, D. F. V. James, T. Shirai, and E. Wolf, “Intensity fluctuations and the degree of cross-polarization in stochastic electromagnetic beams,” *J. Opt. A Pure Appl. Opt.* **10**, 055001 (2008).
11. A. Al-Qasimi, M. Lahiri, D. Kuebel, D. F. V. James, and E. Wolf, “The influence of the degree of cross-polarization on the Hanbury Brown–Twiss effect,” *Opt. Express* **18**, 17124–17129 (2010).
12. T. Hassinen, J. Tervo, T. Setälä, and A. T. Friberg, “Hanbury Brown–Twiss effect with electromagnetic waves,” *Opt. Express* **19**, 15188–15195 (2011).
13. F. Gori, M. Santarsiero, G. Piquero, R. Borghi, A. Mondello, and R. Simon, “Partially polarized Gaussian Schell-model beams,” *J. Opt. A* **3**, 1–9 (2001).
14. Y. Li, “Correlations between intensity fluctuations in stochastic electromagnetic Gaussian Schell-model beams,” *Opt. Commun.* **316**, 67–73 (2014).
15. G. Wu and T. D. Visser, “Hanbury Brown–Twiss effect with partially coherent electromagnetic beams,” *Opt. Lett.* **39**, 2561–2564 (2014).
16. E. Collett and E. Wolf, “Beams generated by Gaussian quasi-homogeneous sources,” *Opt. Commun.* **32**, 27–31 (1980).
17. Y. Li and E. Wolf, “Radiation from anisotropic Gaussian Schell-model sources,” *Opt. Lett.* **7**, 256–258 (1982).
18. E. Wolf and W. H. Carter, “Fields generated by homogeneous and by quasi-homogeneous planar secondary sources,” *Opt. Commun.* **50**, 131–136 (1984).

19. W. H. Carter and E. Wolf, "Inverse problem with quasi-homogeneous sources," *J. Opt. Soc. Am. A* **2**, 1994–2000 (1985).
20. K. Kim and E. Wolf, "Propagation law for Walther's first generalized radiance function and its short-wavelength limit with quasi-homogeneous sources," *J. Opt. Soc. Am. A* **4**, 1233–1236 (1987).
21. J. T. Foley and E. Wolf, "Radiometry with quasi-homogeneous sources," *J. Mod. Opt.* **42**, 787–798 (1995).
22. W. H. Carter and E. Wolf, "Coherence and radiometry with quasi-homogeneous planar sources," *J. Opt. Soc. Am. A* **67**, 785–796 (1977).
23. T. D. Visser, D. G. Fischer, and E. Wolf, "Scattering of light from quasi-homogeneous sources by quasi-homogeneous media," *J. Opt. Soc. Am. A* **23**, 1631–1638 (2006).
24. S. B. Raghunathan, T. D. Visser, and E. Wolf, "Far-zone properties of electromagnetic beams generated by quasi-homogeneous sources," *Opt. Commun.* **295**, 11–16 (2013).
25. E. Wolf, "Unified theory of coherence and polarization of random electromagnetic beams," *Phys. Lett. A* **312**, 263–267 (2003).
26. T. D. Visser, D. Kuebel, M. Lahiri, T. Shirai, and E. Wolf, "Unpolarized light beams with different coherence properties," *J. Mod. Opt.* **56**, 1369–1374 (2009).
27. F. Gori, M. Santarsiero, R. Borghi, and V. Ramírez-Sánchez, "Realizability condition for electromagnetic Schell-model sources," *J. Opt. Soc. Am. A* **25**, 1016–1021 (2008).
28. J. R. Fienup, "Phase retrieval algorithms: a personal tour," *Appl. Opt.* **52**, 45–56 (2013).
29. J. R. Fienup, "Reconstruction of an object from the modulus of its Fourier transform," *Opt. Lett.* **3**, 27–29 (1978).